Molecular motors

DOI: 10.1002/smll.200500223

Transport of Semiconductor Nanocrystals by Kinesin Molecular Motors**

Gayatri Muthukrishnan, Benjamin M. Hutchins, Mary Elizabeth Williams, and William O. Hancock**

Kinesin molecular motors harness the energy of ATP hydrolysis to transport cargo such as vesicles and organelles along intracellular microtubules. Purified components of this system can be used for nanoscale transport by integrating the motors and filaments into MEMS and NEMS devices.[1–4] Hence, it is important to understand the function of these proteins for biological, therapeutic, and nanotechnological applications. Existing techniques for studying motors include the microtubule gliding assay,[5] optical traps,[6] and ATPase assays.[7] Single-molecule visualization is crucial for investigating the motor mechanism and their ability to move and assemble nanoparticles.[8–10] In this report, we synthesize semiconductor nanocrystals, attach them to kinesins, demonstrate that single motors can be visualized by simple epifluorescence or evanescent wave microscopy, and show that motor function is unaffected by particle functionalization.

Single kinesin motors functionalized with green fluorescent protein (GFP) or synthetic fluorophores can be imaged by total internal reflection fluorescence (TIRF) microscopy,[8] and their position resolved to within nearly one nanometer.[11] By tracking kinesins in which one of the two motor domains (heads) was labeled, this technique was used to show that at limiting ATP concentrations each head takes 16-nm steps along a microtubule, ruling out the "inchworm" model of kinesin motility.[11] However, because the spatial resolution is based on the number of photons collected, the temporal resolution using these fluorophores is limited to roughly 300 ms. Brighter fluorophores are needed to measure faster events. While fluorescent beads have higher signal intensities, their size alters the diffusion properties of the tagged molecule and complicates intracellular experiments.

Semiconductor nanocrystals (quantum dots) have great potential in biological imaging due to their small size (≈5–10 nm radius with functionalization), high quantum yield, large excitation band, and negligible photobleaching. Quantum dots with different optical properties can be synthesized with ease by growing them to different sizes,[12] and single fluorophores can be visualized by simple epifluorescence microscopy rather than the evanescent wave microscopy that is generally required for GFP and other synthetic fluorophores. In addition, they can be introduced into cells by a variety of methods.[13] By synthesizing our own quantum dots, we have the advantage of being able to separately tune the emission wavelength and control the surface functionality.

The goal of this study is to functionalize quantum dots with active kinesin biomolecular motors and transport these dots along immobilized microtubules. This new labeling approach will open up a number of avenues of investigation. First, it will enable more precise tracking of motors in vitro to understand motor stepping and detachment under controlled conditions. Second, these bright particles should enable individual kinesins to be followed in cells, which is very difficult with current labeling procedures. Third, quantum dots can be used as models for biomotor-driven nanoparticle assembly in vitro.

More and more materials are being synthesized at nanoscale geometries that confer novel and enhanced functionality. However, despite the success of various self-assembly processes, organization of these nanoparticles into configurations far from their thermodynamic minima is a continuing hurdle. Because kinesins are specialized transport motors that have evolved to organize the intracellular environment, they provide a powerful tool for transport and assembly of synthetic nanomaterials. Harnessing these biological motors for this purpose requires a model system that can be easily visualized and quantified. At present, microtubules that have been coated with quantum dots have been shown to move along immobilized motors so long as the region of functionalization is limited.[14] Furthermore, in a related and impressive recent study, individual myosin V motors were labeled with a different-colored quantum dot on each head to definitively show that the two heads alternately step along an immobilized actin filament.[15] Here, we demonstrate for the first time that individual kinesin motors can be functionalized with quantum dots, and their movement along microtubules easily tracked by either TIRF or epifluorescence microscopy.

Using quantum dots for this purpose comes with a number of hurdles. Generally, quantum-dot cores are synthesized in an organic phase and usually with cytotoxic compounds,[16–18] so for biological applications the cores need to be protected and transferred to an aqueous phase by coating with a shell of a second semiconductor with a larger bandgap and with protective ligands. Additional ligands must be

[*] G. Muthukrishnan, Dr. W. O. Hancock
Department of Bioengineering, 229 Hallowell Bldg.
The Pennsylvania State University
University Park, PA 16802 (USA)
Fax: (+1) 814-863-0490
E-mail: mbw@chem.psu.edu
B. M. Hutchins, Dr. M. E. Williams
Department of Chemistry, 104 Chemistry Bldg.
The Pennsylvania State University
University Park, PA 16802 (USA)
E-mail: mbw@chem.psu.edu

[**] The authors thank Yangrong Zhang and Kihong Ahn for assistance with microscopy and motor visualization, Jeff Gelles (Brandeis University) for the gift of the K401-bio plasmid, and Zachary Donhauser for making the His-tagged K401-bio construct. This work was supported by The Pennsylvania State University Center for Nanoscale Science, a NSF Materials Research Science and Engineering Center (DMR0213623).

Supporting information for this article is available on the WWW under http://www.small-journal.com or from the author.

added to the surface of the quantum dot to enable motor attachment while preventing aggregation. Direct covalent chemistry or, as shown here, biotin–avidin can be used to link the motors to quantum dots.

To maximize single-motor labeling and minimize aggregation, quantum dot–kinesin (Q–kin) complexes (Figure 1)

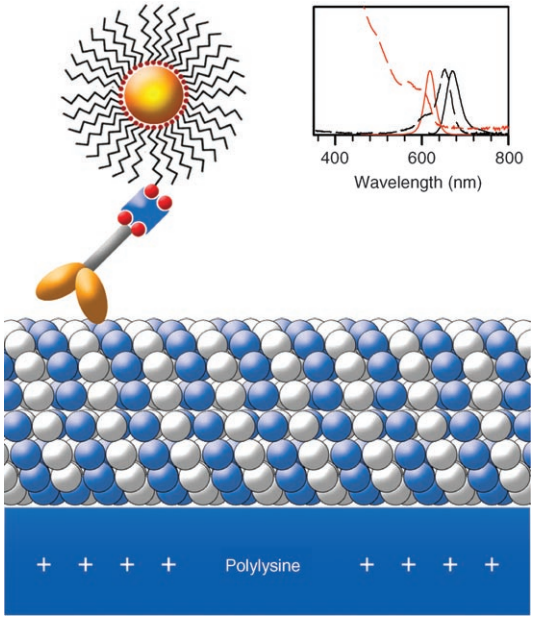

Figure 1. Schematic of a kinesin–neutravidin–quantum dot complex moving along a surface-immobilized microtubule. Molecules are drawn approximately to scale, the microtubule is 24 nm in diameter and the core/shell quantum dot is 7.6 nm in diameter. Inset: absorbance (– – –) and emission (——) spectra of quantum dots (in red) synthesized and used in this investigation; Alexa Fluor 647-labeled microtubules (in black).

were assembled using a 0.2:5:1 ratio of biotinylated kinesin/neutravidin/quantum dots. Kinesin motility was observed using the Q–kin motility assay (see Experimental Section) and in parallel experiments, motors were investigated using the microtubule gliding and bead assays.[19,20]

The motors were visualized by both TIRF and epifluorescence microscopy with similar results (Figure 2). The evanescent excitation in TIRF reduced the background fluorescence, but the tradeoff was that only binding events to microtubules that were tightly adhered to the surface, and thus within the thin evanescent wave, were visualized. However, it was found that a large fraction of the motor–microtubule interactions occur on weakly bound microtubules both in this study and when motors are adsorbed to 0.2-μm silica beads.[21] Epifluorescent illumination also enabled visualization of the moving quantum dots. Because this mode is more widely used and easier to implement than TIRF, quantum-dot functionalization of kinesins should lower the bar for performing single-molecule kinesin observations.

In standard kinesin assays using fluorescent microtubules, an antifade cocktail consisting of an oxygen-scavenging system (20 mM glucose, 0.02 mg mL^{-1} glucose oxidase, 0.008 mg mL^{-1} catalase) and reducing agent (75 mM β-mercaptoethanol) is required to prevent free-radical-induced fluorophore bleaching and protein degradation. In a recent report, Hohng and Ha found that adding 140 mM β-mercaptoethanol to quantum dots in TE Buffer (10 mM Tris-HCl, 1 mM EDTA, pH 7.5) virtually eliminated blinking, which led to a higher time-averaged fluorescence.[22] In contrast, even in our best preparations, reducing agents did not eliminate blinking, and a portion of the quantum dots were quenched when added to the motility solution. To quantify this effect, we immobilized quantum dots on a glass cover slip, passed buffers with and without β-mercaptoethanol over them, and counted the number of emissive particles. Addition of β-mercaptoethanol caused a reduction in the number of observable dots to 19.7 ± 6.9 % (mean ± standard deviation (SD) from 5 flow cells) in BRB12 buffer and to similar levels in BRB80 and TE buffer. Blinking was observed in all cases, and the remaining dots were apparently unaffected by the reducing agent. Hence, β-mercaptoethanol quenches a subset of the quantum dots, presumably due to defects in the protective shell, but does not suppress blinking. Thiols are known to cause surface traps on CdSe particles, where the thiol binding site becomes a trap site, and promotes the formation of a disulfide that then dissociates and leaves a nonluminescent particle.[23] The penetration of a small thiol molecule (such as β-mercaptoethanol) into a shell defect site would presumably be sufficient to cause the total quenching of a quantum dot with available shell defects. Although this phenomenon appears not to affect the remaining quantum dots, this result has important implications for future studies that combine reducing agents and quantum dots.

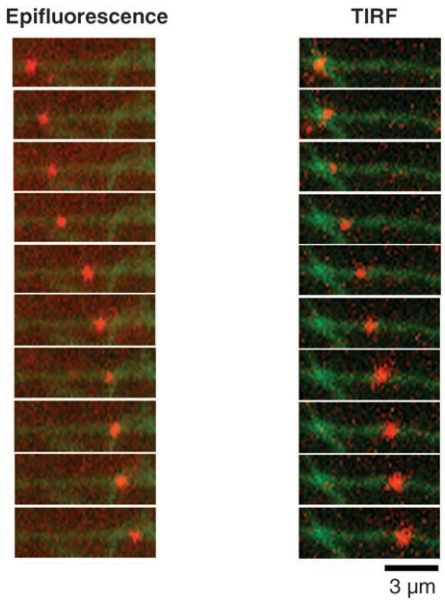

Figure 2. Microscopic assay showing a quantum dot–kinesin complex moving along an immobilized fluorescently labeled microtubule. Images on the left are in epifluorescence mode (elapsed time = 13 s); images on the right are in TIRF mode (elapsed time = 20 s).

To analyze motor function, the first metric measured was the motor run length, that is, the distance motors

moved along microtubules before detaching and diffusing away. This was achieved by monitoring all dots that bound to the microtubule surface and measuring the axial displacement of those that moved a minimum of 0.5 μm. At the ratio of 0.2 kinesins per quantum dot, the run length was exponentially distributed with an average of 2.11 ± 0.18 μm (exponential fit mean ± standard error (SE), number of events (N) = 81; Figure 3A), and at 2 kinesins per quantum

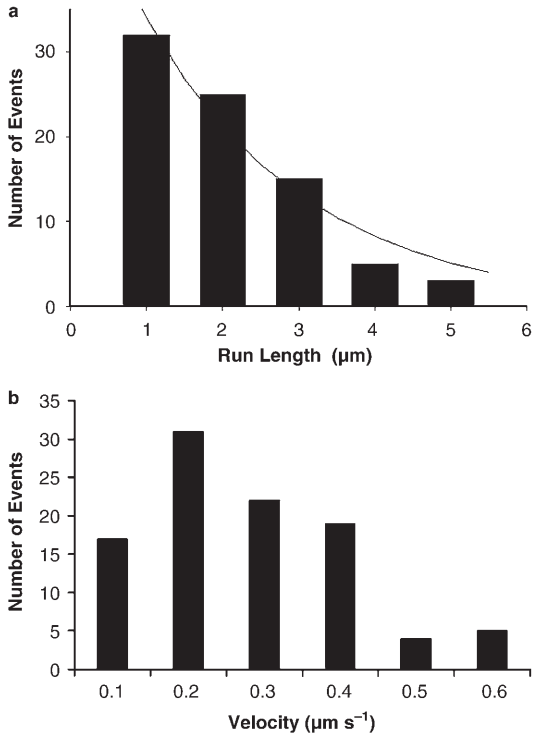

Figure 3. Run length and velocity of quantum dot–kinesin conjugates (0.2 kinesins per quantum dot) measured for events over three flow cells: a) Run lengths of 81 events are fit to a single exponential curve, neglecting values below 0.5 μm because of uncertainty in detecting all of these short events. The exponential fit gave a mean run length of 2.11 μm. b) Velocity distribution including all observed events. Mean velocity ± SD was 0.28 ± 0.12 μm s^{-1} (N = 101).

dot, the run length was 2.46 ± 0.15 μm (N = 101). These numbers are slightly higher than some reported measurements of individual kinesin motors attached to submicrometer silica beads[6,20] or fused to GFP,[24,25] but match the 2.3 ± 0.7 μm run length reported for a very similar biotinylated *Drosophila* kinesin construct bound to silica beads.[26] When our biotinylated motors were attached to neutravidin-coated 0.2-μm-diameter silica beads at 20 kinesins per bead, the measured run lengths were 2.92 ± 0.16 μm (N = 96; see Supporting Information). These results suggest that the movement of the Q–kin complexes is driven by individual kinesin motors and that a single biochemical transition determines the detachment of the motor from the microtubule.

The second motor parameter analyzed was the transport velocity, an indicator of the stepping frequency and ATP hydrolysis rate of the motor. In standard microtubule gliding assays in BRB12 buffer, these biotinylated kinesin motors moved microtubules at speeds of 0.17 ± 0.03 μm s^{-1} (mean ± SD, N = 50). This speed is slower than the 0.56 ± 0.04 μm s^{-1} (N = 50) measured in BRB80 buffer, but the lower ionic strength is chosen to maximize motor–microtubule interactions in the quantum-dot assays. When standard bead assays were performed by attaching biotinylated kinesins to neutravidin-labeled 0.2-μm silica beads, the mean bead velocity was 0.33 ± 0.08 μm s^{-1} (N = 50). Kinesin-functionalized quantum dots at 0.2 kinesins per quantum dot moved at 0.28 ± 0.12 μm s^{-1} (N = 101; Figure 3B), and dots with 2 kinesins per quantum dot moved at 0.26 ± 0.11 μm s^{-1} (N = 101). Thus, attaching quantum dots to these biotinylated kinesins does not compromise motor function.

Lastly, to demonstrate the potential for long-term imaging, Q–kin complexes were bound to immobilized microtubules (in the presence of the non-hydrolyzable nucleotide analog AMP-PNP) on to glass surfaces, illuminated continuously by evanescent excitation at 488 nm, and monitored over time. The mean time that particles could be continuously visualized was > 1200 s, which we regard as a lower limit due to motor unbinding and eventual microtubule depolymerization. This duration is nearly two orders of magnitude longer than the ≈ 17 s or ≈ 12 s that Cy3[27,28] or GFP-labeled kinesin[25] can be imaged before photobleaching. Quantum-dot labeling should therefore eliminate the need for correcting estimates for motor run lengths due to photobleaching events.[25]

Hence, by conjugating quantum dots to motors through biotin–avidin, these semiconductor nanocrystals can be used as bright and robust fluorophores to track conventional kinesin movement along cytoskeletal filaments. With further optimization of quantum-dot conjugate preparation techniques, these labels can potentially be used to image other members of the 13 families of kinesins as well as other molecular motors. Additionally, because of their small size and bright fluorescence, the quantum dots can be used for in vitro investigations of biomotor-driven nanoparticle transport and organization along the microtubule lattice. Such motor-driven organization should be much more deterministic than simple diffusion, surface force-mediated aggregation, or other self-assembly approaches. Finally, because these particles can be synthesized with a range of emission properties and surface chemistries, they can be used to investigate bidirectional transport by motors and co-assembly of heterogeneous particles.

Experimental Section

Protein preparations: *Drosophila melanogaster* conventional heavy-chain kinesin plasmid[29] was modified by deleting the tail and coiled-coil domains (cut at site corresponding to amino acid 401) and adding sequences for the biotin carboxyl carrier protein (BCCP)[30] and hexa-histidine tag. The recombinant protein was expressed in *Escherichia coli* BL21(DE3) cells and purified by Ni-NTA affinity chromatography using an Amersham Biosciences FPLC system following established procedures.[19] Kinesin concentration was quantified by gel densitometry using a UVP BioChemi System (UVP, Inc., Upland, CA) and SyproRed protein

stain (Molecular Probes, Invitrogen) using bovine serum albumin as a standard. Tubulin was purified from calf brains and labeled with Alexa Fluor 647 carboxylic acid succinimidyl ester (Molecular Probes, Invitrogen) according to standard techniques.[31,32] Microtubules were polymerized for 20 min at 37 °C in the presence of GTP (1 mM), $MgCl_2$ (4 mM), and DMSO (5%), and stabilized by diluting into a solution of paclitaxel (10 μM) in BRB80 buffer (80 mM PIPES, 1 mM $MgCl_2$, 1 mM EGTA, pH 6.8).

Quantum dot synthesis: CdSe/ZnS core/shell quantum dots were synthesized by published methods[33] and functionalized with biotin. The recently reported successive ion layer adsorption and reaction (SILAR) technique was used to impart a three-monolayer protective ZnS shell.[34,35] CdSe/ZnS particles were transferred to an aqueous phase and biotinylated by introducing polyethylene oxide phospholipid (DSPE-PEG(2000), Avanti Polar Lipids, Inc.) which preferentially forms a protective micelle structure.[36] We used a mixed micelle solution of 1% biotin-terminated phospholipid (DSPE-PEG(2000)Biotin), the rest being methoxy-terminated phospholipid. See the Supporting Information for further details on quantum-dot synthesis and functionalization.

Quantum dot–kinesin (Q–kin) conjugation: The biotinylated kinesin (7.2 nM) was first incubated with neutravidin (180 nM; Pierce Biotechnology, Inc.) for 5 min in BRB12 buffer (12 mM PIPES, 2 mM $MgCl_2$, 1 mM EGTA, pH 6.8) containing MgATP (1 mM). We chose BRB12 buffer for this study because at lower ionic strengths the motor–microtubule on-rate is higher, leading to more observable events. Subsequently, biotinylated quantum dots (36 nM) were added and incubated for 20 min. Finally, a tenfold excess of free biotin was added to block any free biotin-binding sites on neutravidin, and the complex centrifuged in a Beckman Airfuge for 10 min at 30 psi (≈95 000 rpm or 178 000 × g) to remove any aggregates.

Q–kin motility assay: Glass cover slips (Corning Cover Glass, 18 mm Squares, No. $1^1/_2$) were treated with 2 M KOH for 30 min, rinsed in distilled water, then incubated in a 0.1% poly-L-lysine solution for 30 min, rinsed extensively in water, and dried. In contrast to aminosilane-treated surfaces, which adsorbed quantum dots to the point where measurement of moving particles was nearly impossible, nonspecific binding to the casein-coated poly-L-lysine-treated surface was minimal (limited to 5–10 per 760 μm^2 screen). Flow cells were constructed from a cover slip, a microscope slide, and two-sided tape. Microtubules (0.06 μM tubulin dimer) were introduced and incubated for 5 min, and the surface was then blocked with a solution of casein (5 mg mL^{-1}) and paclitaxel (10 μM) in BRB12 buffer. Finally, a solution of Q–kin conjugates in motility buffer (10 μM paclitaxel, 0.2 mg mL^{-1} casein, 1 mM ATP, 20 mM glucose, 0.02 mg mL^{-1} glucose oxidase, 0.008 mg mL^{-1} catalase, 0.5% β-mercaptoethanol in BRB12) was introduced into the flow cell (Figure 1).

Microtubule gliding assay: The microtubule gliding assay was performed according to published procedures,[19] except that instead of adsorption of full-length kinesin directly to the glass, 1 mg mL^{-1} neutravidin was adsorbed to the glass and biotinylated motors were bound to the neutravidin. The motility of Alexa Fluor 647-labeled microtubules in BRB12 motility buffer was observed.

Bead assay: Neutravidin-coated beads were prepared by incubating 0.2-μm-diameter silica beads (1 nM; Bangs Laboratories, Inc.) with neutravidin (0.4 mg mL^{-1}) for 15 min in BRB80 while sonicating. Subsequently, rhodamine-labeled casein (0.4 mg mL^{-1}) and unlabeled casein (4 mg mL^{-1}) were added to the bead solution, the mixture was sonicated for one hour, and the beads were centrifuged for 5 min at 18 400 × g to remove excess neutravidin and rhodamine–casein from the solution. Beads were functionalized with biotinylated kinesin by incubating motors (1 nM or 2 nM) with beads (100 pM) for 10 min in BRB12 with casein (5 mg mL^{-1}) and ATP (1 mM). Alexa Fluor 647-labeled microtubules were immobilized on the poly-L-lysine surface and the surface blocked similar to the Q–kin motility assay. For motility measurements the kinesin-coated beads were diluted to 50 pM in BRB12 motility buffer, introduced into the flow cell, and visualized by fluorescence microscopy.

Microscopic visualization: Fluorescent microtubules and quantum dots were observed both under epifluorescence and TIRF using a Nikon TE2000 inverted microscope (60×, 1.45 NA, CFI Plan Apo TIRF oil objective), and imaged using a Photometrics Cascade 512B CCD camera (Roper Scientific). The camera was controlled and images acquired using Meta-Vue software (Universal Imaging, PA) run on a PC. Stacks of images were captured with 50 ms or 100 ms acquisition times and analyzed for motor velocities and run lengths. Silica beads were visualized by epifluorescence on a Nikon E600 upright microscope (100×, 1.3 NA objective) with a Genwac GW-902H CCD camera, recorded by video, and analyzed off-line.

Curve fitting: Exponential run length data were fit to the cumulative probability function

$$P(x) = 1 - \exp(-(x - x_0)/\lambda)$$

where $P(x)$ is the probability of the motor detaching at or before distance x, x_0 is the minimum distance measured (0.5 μm), and λ is the mean run length in μm.[25] This method was chosen because it removes variability due to choice of bin width. When 1-μm bin widths were used and the Q–kin data fit to a single exponential with no weighting, the run lengths were within 5% of the cumulative fit. Data fitting was performed using SigmaPlot 8.0 (Systat Software, Inc., Point Richmond, CA).

Keywords:

biomolecular motors · bionanotechnology · biophysics · molecular imaging · quantum dots

[1] S. G. Moorjani, L. Jia, T. N. Jackson, W. O. Hancock, *Nano Lett.* **2003**, *3*, 633–637.
[2] H. Hess, J. Clemmens, D. Qin, J. Howard, V. Vogel, *Nano Lett.* **2001**, *1*, 235–239.
[3] J. R. Dennis, J. Howard, V. Vogel, *Nanotechnology* **1999**, *10*, 232–236.
[4] Y. Hiratsuka, T. Tada, K. Oiwa, T. Kanayama, T. Q. Uyeda, *Biophys. J.* **2001**, *81*, 1555–1561.
[5] J. Howard, A. J. Hudspeth, R. D. Vale, *Nature* **1989**, *342*, 154–158.
[6] S. M. Block, L. S. Goldstein, B. J. Schnapp, *Nature* **1990**, *348*, 348–352.
[7] D. D. Hackney, *Proc. Natl. Acad. Sci. USA* **1988**, *85*, 6314–6318.

[8] D. W. Pierce, R. D. Vale, *Methods Enzymol.* **1998**, *298*, 154 – 171.
[9] J. Yajima, M. C. Alonso, R. A. Cross, Y. Y. Toyoshima, *Curr. Biol.* **2002**, *12*, 301 – 306.
[10] M. Platt, G. Muthukrishnan, W. O. Hancock, M. E. Williams, *J. Am. Chem. Soc.* **2005**, *127*, 15 686 – 15 687.
[11] A. Yildiz, M. Tomishige, R. D. Vale, P. R. Selvin, *Science* **2004**, *303*, 676 – 678.
[12] C. B. Murray, D. J. Norris, M. G. Bawendi, *J. Am. Chem. Soc.* **1993**, *115*, 8706.
[13] A. M. Derfus, W. C. W. Chan, S. N. Bhatia, *Adv. Mater.* **2004**, *16*, 961 – 966.
[14] G. D. Bachand, S. B. Rivera, A. K. Boal, J. Gaudioiso, J. Liu, B. C. Bunker, *Nano Lett.* **2004**, *4*, 817 – 821.
[15] D. M. Warshaw, G. G. Kennedy, S. S. Work, E. B. Krementsova, S. Beck, K. M. Trybus, *Biophys J.* **2005**, *88*, L30 – L32.
[16] A. M. Derfus, W. C. W. Chan, S. N. Bhatia, *Nano Lett.* **2004**, *4*, 11 – 18.
[17] A. Hoshino, K. Fujioka, T. Oku, S. Masakazu, Y. F. Sasaki, T. Ohta, M. Yasuhara, K. Suzuki, K. Yamamoto, *Nano Lett.* **2004**, *4*, 2163 – 2169.
[18] A. Shiohara, A. Hoshino, K. Hanaki, K. Suzuki, K. Yamamoto, *Microbiol. Immunol.* **2004**, *48*, 669 – 675.
[19] W. O. Hancock, J. Howard, *J. Cell Biol.* **1998**, *140*, 1395 – 1405.
[20] W. O. Hancock, J. Howard, *Proc. Natl. Acad. Sci. USA* **1999**, *96*, 13 147 – 13 152.
[21] W. O. Hancock, The Pennsylvania State University, **2004**, unpublished results.
[22] S. Hohng, T. Ha, *J. Am. Chem. Soc.* **2004**, *126*, 1324 – 1325.
[23] J. Aldana, Y. A. Wang, X. Peng, *J. Am. Chem. Soc.* **2001**, *123*, 8844 – 8850.
[24] L. Romberg, D. W. Pierce, R. D. Vale, *J. Cell Biol.* **1998**, *140*, 1407 – 1416.
[25] K. S. Thorn, J. A. Ubersax, R. D. Vale, *J. Cell Biol.* **2000**, *151*, 1093 – 1100.
[26] Y. Vugmeyster, E. Berliner, J. Gelles, *Biochemistry* **1998**, *37*, 747 – 757.
[27] D. W. Pierce, N. Hom-Booher, R. D. Vale, *Nature* **1997**, *388*, 338.
[28] S. Lakamper, A. Kallipolitou, G. Woehlke, M. Schliwa, E. Meyhofer, *Biophys. J.* **2003**, *84*, 1833 – 1843.
[29] D. L. Coy, M. Wagenbach, J. Howard, *J. Biol. Chem.* **1999**, *274*, 3667 – 3671.
[30] J. E. Cronan, *J. Biol. Chem.* **1990**, *265*, 10 327 – 10 333.
[31] R. C. Williams, Jr., J. C. Lee, *Methods Enzymol.* **1982**, *85*, 376 – 385.
[32] A. Hyman, D. Drechsel, D. Kellogg, S. Salser, K. Sawin, P. Steffen, L. Wordeman, T. Mitchison, *Methods Enzymol.* **1991**, *196*, 478 – 485.
[33] L. Qu, Z. A. Peng, X. Peng, *Nano Lett.* **2001**, *1*, 333 – 337.
[34] J. J. Li, Y. A. Wang, W. Guo, J. C. Keay, T. D. Mishima, M. B. Johnson, X. Peng, *J Am. Chem. Soc.* **2003**, *125*, 12 567 – 12 572.
[35] R. Xie, U. Kolb, J. Li, T. Basche, A. Mews, *J Am. Chem. Soc.* **2004**, *127*, 7481 – 7488.
[36] B. Dubertret, P. Skourides, D. J. Norris, V. Noireaux, A. H. Brivanlou, A. Libchaber, *Science* **2002**, *298*, 1759 – 1762.

Received: July 6, 2005
Revised: November 8, 2005

